JOURNAL OF FOOD AND DRUG ANALYSIS 25 (2017) 976–983

Available online at www.sciencedirect.com

ScienceDirect

journal homepage: www.jfda-online.com

Original Article

Phosphorylation and antiaging activity of polysaccharide from *Trichosanthes* peel

Min Zhang [a,1], *Nana Su* [a,1], *Qianli Huang* [b], *Qiang Zhang* [a,c], *Yufen Wang* [a], *Jinglei Li* [a,*], *Ming Ye* [a,*]

[a] *School of Food Science and Engineering, Hefei University of Technology, Hefei, China*
[b] *School of Biological and Medical Engineering, Hefei University of Technology, Hefei, China*
[c] *College of Biological Science and Engineering, Beifang University of Nationalities, Yinchuan, China*

ARTICLE INFO

Article history:
Received 31 August 2016
Received in revised form
14 December 2016
Accepted 19 December 2016
Available online 13 February 2017

Keywords:
antiaging activity
phosphorylation modification
Trichosanthes peel polysaccharide

ABSTRACT

Polysaccharides from *Trichosanthes* peel (TPP) were obtained by ultrasound-assisted extraction. TPP-1 was separated from the TPP by Sephadex G-100 column chromatography. Phosphorylation of TPP-1 was carried out and phosphorylated TPP-1 was named as PTTP-1. The results of infrared spectra, ^{13}C nuclear magnetic resonance spectra and ^{31}P nuclear magnetic resonance spectra showed that the main structure of PTPP-1 was similar to that of TPP-1 and -H_2PO_3 groups which were conjugated to C-6 of →4)-α-D-Man*p*-(1→, C-4 of →6)-α-D-Gal*p*-(1→, C-2 and C-3 of →1)-α-L-Ara*f*, C-2 of →1)-α-L-Ara*f*-(3→, and C-6 and C-3 of →1)-α-D-Glc*p*. *In vivo* antiaging activity results proved that TTP-1 and PTTP-1 could both significantly improve the body weight, spleen index, and thymus index of the D-galactose-induced aging mice, increase the levels of superoxide dismutase, catalase, glutathione peroxidase, and reduce malondialdehyde contents in the liver, brain, and serum of aging mice. These results indicated that both TPP-1 and PTTP-1 presented significant antiaging activity. Moreover, PTTP-1 showed stronger antiaging effects in aging mice, indicating that phosphorylation improved antiaging effect.

1. Introduction

Aging is a degenerative change process of tissue and organ functions of bodies along with the age growth. Oxidative stress is considered as the primary cause for senescence, generation of oxidative stress, cytomembrane damage, degeneration of proteins and enzymes, and even induction of cellular apoptosis and induced as free radical levels increase [1]. Once oxidative damage caused by free radicals overwhelms the body's repair ability, it will lead to the change or even loss of cell's differentiation, thereby accelerating the aging process [2]. Along with the aging tendency of the worldwide population, people are beginning to pay more attention to studies on development of antioxidative and antiaging drugs [3]. Modern pharmacological investigations have indicated that active polysaccharides derived from plants have distinct antioxidative and antiaging effects [4,5].

* *Corresponding authors*. School of Food Science and Engineering, Hefei University of Technology, Heifei 230009, China.
E-mail addresses: lijinglei2010@hotmail.com (J. Li), yeming123@sina.com (M. Ye).
[1] Min Zhang and Nana Su contributed equally to this work.
http://dx.doi.org/10.1016/j.jfda.2016.12.013

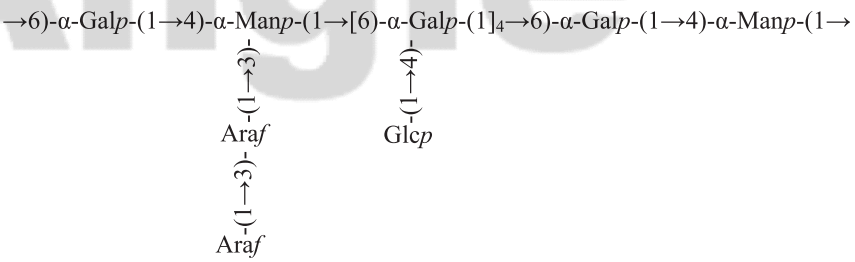

Figure 1 – The proposed structure of TPP-1.

Plant polysaccharide is a kind of polymer composed of multiple monosaccharides and is one kind of biomacromolecule showing extensive bioactivities [6–9]. Plant polysaccharide, as a kind of immunomodulator, carried distinct antiaging effects [10,11]. Plant polysaccharides might exert their antiaging activity by improving the superoxide dismutase (SOD), catalase (CAT), and glutathione peroxidase (GSH-PX) activities, reducing the malondialdehyde (MDA) content, restraining the monoamine oxidase activity, regulating the protein, nucleic acid, sugar, and lipid metabolism, and inhibiting the lipid peroxidation and lipofusion generation [12]. The activities of polysaccharide were related to the composition of monosaccharide residues, categories of glycosidic linkage, the degree of polymerization, branching coefficient as well as the flexibility and configuration of backbones and branches.

Certain natural polysaccharides were modified through phosphorylation, sulfation and carboxymethylation to alter their structures and promote their bioactivities. Previously, Liu et al. [13] reported that phosphorylated and sulfated derivatives exhibited significant antiherpetic activity of *Polygonatum cyrtonema* Hua polysaccharide, whereas acetylated and carboxymethylated derivatives were shown to be almost inactive. Sinha et al. [14] reported that sulfation could improve the antiviral activities of *Sargassum tenerrimum* polysaccharide. Phosphorylated polysaccharide has stronger immunocompetence, anticoagulation, and antineoplastic activity than the natural polysaccharide [15–17].

Trichosanthes kirilowii Maxim is widespread in the East Asia and northern Australia. *Trichosanthes* pericarp is the peel of the matured *Trichosanthes* fruits which is rich in grease, organic acid, polysaccharide, flavones, protein, etc. [18]. It was reported that *Trichosanthes* peel was widely used in traditional Chinese medicine to treat diseases of cerebrovascular, cardiovascular, and respiration systems due to its abilities to clear heat and dissipate phlegm, regulate the flow of vital energy, and relieve chest stuffiness [19,20]. Our recent studies showed that one homogeneous polysaccharide (TPP-1) separated from *Trichosanthes* peel polysaccharide (TPP) was a kind of heteroglycan. The backbone of TPP-1 was composed of →6)-α-D-Gal*p*-(1→, →4)-α-D-Man*p*-(1→, →1)-α-D-Man*p*-(3,4→ and →1)-α-D-Gal*p*-(4,6→, while the branches were consisted of →1)-α-D-Glc*p*, →1)-α-L-Ara*f* -(3→ and →1)-α-L-Ara*f*. The proposed structure of TPP-1 was shown in Figure 1.

However, there is no report on the structure and bioactivities of phosphorylated TPP-1. This study focused on phosphorylation modification of TPP-1 and the antiaging activity of the polysaccharide before and after the modification.

2. Materials and methods

2.1. Materials

Trichosanthes (*T. kirilowii* Maxin) peel was provided by Lushi Ecological Agricultural Technology Co., Ltd (Anhui, China). The homogeneous heteroglycan, TPP-1, was separated from TPP by Sephadex G-100 column chromatography and preserved in Microbial Resource and Application Research Center, Hefei University of Technology.

2.2. Laboratory animals

Eighty-four Kunming mice (42 male and 42 female), with weight of 20 ± 2 g, were purchased from the Laboratory Animal Center, Anhui Medical University with the number of conformity certificate: No. 1 license of the Medical Laboratory Animal of Anhui. Growth conditions: temperature 23 ± 2°C, humidity 55 ± 5%, alternative feeding at 14 hours of light and 10 hours of darkness.

All animals' treatments were strictly in accordance with the National Institutes of Health Guide for the Care and Use of Laboratory Animals.

2.3. Reagents and instruments

SOD, CAT, GSH-PX, and MDA kits were purchased from Nanjing Jiancheng Technology Co., Ltd (Nanjing, China). D-galactose (Sigma, Louis, Missouri, USA). Instruments used Fourier transform infrared (FTIR) spectrometer Nexus670 (Thermo Nicolet, Manhattan, New York, USA), the nuclear magnetic resonance (NMR) Bruker Avance AV500 (Bruker,

Table 1 – ^{13}C nuclear magnetic resonance chemical shift (unit: ppm) data of polysaccharides from *Trichosanthes* peel (TPP-1).

Residue	C-1	C-2	C-3	C-4	C-5	C-6
→6)-α-D-Gal*p*-(1→	101.65	78.14	72.74	**66.32**	70.59	66.41
→4)-α-D-Man*p*-(1→	100.03	74.89	72.56	69.72	76.28	**60.52**
→1)-α-D-Man*p*-(3,4→	100.03	74.99	72.11	69.41	72.74	62.21
→1)-α-D-Glc*p*	97.65	75.84	**75.91**	72.74	75.00	**69.49**
→1)-α-D-Gal*p*-(4, 6→	98.79	80.41	75.00	72.74	70.29	61.93
→1)-α-L-Ara*f* -(3→	106.53	**80.81**	87.66	82.23	65.99	—
→1)-α-L-Ara*f*	107.14	**82.23**	**76.28**	87.66	64.94	—

Bold means the carbon chemical shifts might be substituted.

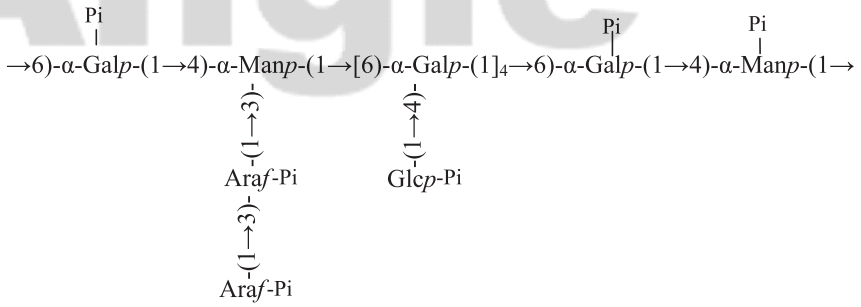

Figure 2 – The proposed structure of PTPP-1.

Munich, Bavaria, Germany) and ELISA iMark (BioRad, Hercules, CA, USA).

2.4. *Preparation of phosphorylated polysaccharide*

The phosphorylation of *Trichosanthes* peel polysaccharide was performed mainly according to method of Ye et al. [21], with some modification. Sodium tripolyphosphate (8.57 g) and 1.43 g of sodium trimetaphosphate were weighed precisely and diluted with double distilled water to 100 mL. TPP-1 (1 g) was added and $NaHCO_3$ was used to adjust the pH to 9. The solution was reacted for 5 hours at 80°C and then was injected to four-fold volume of 95% ethanol to precipitate for 24 hours. Subsequently, the alcohol-precipitated polysaccharide was centrifuged and freeze-dried to obtain powder that was redissolved into 60°C water. After it was dialyzed for 24 hours in a dialysis bag, the lyophilization was carried out to obtain the powder of phosphorylated polysaccharide (PTPP-1).

2.5. *Determination of phosphate radical content in PTPP-1*

Standard curve of phosphate radical: 0 mL, 0.5 mL, 1 mL, 1.5 mL, 2 mL, 2.5 mL, 3 mL, 3.5 mL, 4 mL, 4.5 mL, and 5 mL of phosphate standard liquid (0.1 mg/mL) were sucked up into the tube and then distilled water was injected to 5 mL. Tris buffer solution (3 mL) and 3 mL of phosphorus quantitative reagent were added and reacted for 30 minutes at 45°C [22]. Later, the absorbance at 580 nm (Spectrophotometer 722) was determined. The standard curve of phosphate radical were mapped by taking the absorbance as the ordinate and phosphate radical concentration as the abscissa [23].

The method of Sun et al. [23] was followed to determine the phosphate radical. Lyophilized sample (0.1 g) was added into the tube (containing 1 mL concentrated sulfuric acid and 1 mL concentrated nitric acid) and heated until smoke was seen. Then chilled, added with 1 mL H_2O_2 solution (30%), and heated slowly, and repeated until there were no smoke and the solution was faint yellow or colorless and transparent. Hydrochloric acid (6M, 1 mL) was added and heated for reaction thoroughly. Later, the reaction solution was transferred to a 50-mL volumetric flask, diluted with distilled water. Then, the absorbance was determined according to the abovementioned standard curve method and finally the phosphate radical content was calculated.

2.6. *Infrared spectra of TPP-1 and PTPP-1*

TPP-1 (2 mg) and PTPP-1 (2 mg) were taken respectively and pressed to pellets after being grinded with dried KBr power. Fourier transform infrared spectrometer (Nexus670) was used for IR spectra analysis within the scanning area from 4000/cm to 400/cm.

2.7. *NMR spectra of TPP-1 and PTPP-1*

TPP-1 and PTPP-1 were taken respectively and dissolved into 1.0 mL of D_2O. The NMR spectroscopy Bruker AV-500 was used for ^{13}C NMRanalysis.

Table 2 – Effects on aging mice body weight and organ index of polysaccharides from *Trichosanthes* peel (TPP). A = normal control group; B = negative control group; C = low-dose of TPP-1 group (100 mg/kg); D = high-dose of TPP-1 group (400 mg/kg); E = low-dose of PTPP-1 group (100 mg/kg); F = high-dose of PTPP-1 group (400 mg/kg); G = positive control group.

Group	Weight gain rate (%)	Spleen index (mg/g)	Thymus index (mg/g)	Liver index (mg/g)	Heart index (mg/g)	Kidney index (mg/g)
A	4.62 ± 0.28^{b}	5.85 ± 0.97^{b}	3.27 ± 0.40^{b}	5.79 ± 0.21^{b}	3.79 ± 0.15^{b}	4.23 ± 0.12^{b}
B	1.77 ± 0.19	3.28 ± 0.52	1.18 ± 0.25	3.27 ± 0.16	1.27 ± 0.09	2.28 ± 0.28
C	2.21 ± 0.76	4.16 ± 0.64^{a}	1.52 ± 0.35	4.01 ± 0.26^{a}	2.01 ± 0.10	3.08 ± 0.35^{a}
D	2.96 ± 0.84^{a}	4.84 ± 0.67^{b}	2.05 ± 0.23^{a}	4.19 ± 0.20^{b}	2.19 ± 0.36^{b}	3.15 ± 0.25^{b}
E	3.01 ± 0.82^{b}	5.18 ± 0.87^{b}	2.64 ± 0.40^{b}	4.84 ± 0.11^{b}	2.84 ± 0.32^{b}	3.64 ± 0.17^{b}
F	3.95 ± 0.92^{b}	5.34 ± 0.67^{b}	2.97 ± 0.23^{b}	4.97 ± 0.14^{b}	2.97 ± 0.27^{b}	3.97 ± 0.41^{b}
G	4.22 ± 0.70^{b}	5.63 ± 0.66^{b}	3.15 ± 0.23^{b}	5.63 ± 0.44^{b}	3.63 ± 0.39^{b}	4.12 ± 0.49^{b}

$^{a}p < 0.05$, $^{b}p < 0.01$, compared with the negative control group.

2.8. Antiaging activity

2.8.1. Establishment of aging mice model

The method of Woo et al. [24] was used with minor modification to establish the aging mice model. Healthy Kunming mice were adaptively fed for one week and weighed. The aging mice model was induced by intraperitoneally injection of 2% D-galactose aqueous solution at the dose of 100 mg/kg for consecutive 6 weeks. Afterwards, the experimental mice showed significant aging features such as thin and weak figure and depressed mental state, which indicated that the D-galactose-induced aging mice model was established successfully.

2.8.2. Grouping and drug administration

Sixty D-galactose-induced aging mice were divided randomly into six groups (10 mice per group), including: the D-galactose model control group (10 mL/kg normal saline), positive control group (using vitamin C as the positive drug, 100 mg/kg), TPP-1 low-dose group (100 mg/kg), TPP-1 high-dose group (400 mg/kg), PTPP-1 low-dose group (100 mg/kg) and PTPP-1 high-dose group (400 mg/kg). Another 10 healthy mice were selected as the normal control group (10 mL/kg normal saline). All the experimental mice were administered drugs intragastrically once per day for consecutive 30 days. Mice were weighed again at 24 hours after the last drug administration and their orbital blood was taken and these mice were sacrificed finally by cervical vertebra dislocation.

2.8.3. Determination of visceral indexes

The visceral tissue of the mice was thoroughly cleaned and weighed with the moisture absorbed.

$$\text{Visceral index} = \text{visceral mass/body mass} \times 100\%$$

2.8.4. Determination of SOD, GSH-PX and CAT activities and MDA contents

Blood was collected and centrifuged at 823 *g* for 5 minutes to obtain serum. A 200-mg sample of spleen and 200 mg of thymus tissue of the mice were taken and put in normal saline (2.8 mL) to prepare 10% tissue homogenate, respectively. Afterwards, the tissue homogenate was centrifuged at 823 *g* for 5 minutes to obtain the supernatant. The SOD, GSH-PX, and CAT activities and the content of MDA in the serum, liver homogenate, and cerebral homogenate of the mice were determined. The Unit of Measurement (UOM) of activity was expressed as U/mg protein, while the UOM of MDA content was expressed as nmol/mg protein.

2.9. Statistical analysis

All the data are presented as the mean value ± standard deviation after statistical analysis. Statistical software SPSS13.0 was used for test and variance analysis for intergroup difference. $^{a}p < 0.05$ represents significant difference and $^{b}p < 0.01$ denotes extremely significant difference.

3. Results and discussion

We prepared the derivatives of TPP-1, named as PTPP-1, by sodium trimetaphosphate and sodium tripolyphosphate in the presence of sodium hydroxide. According to the regression equation of phosphate group ($y = 0.0977x + 0.0560$, $R^2 = 0.9991$), the content of PO_4^{3-} in PTPP-1 was calculated as 14.36%. The degree of substitution (DS), designed as the average number of phosphate group ($-H_2PO_3$) on each sugar residue, can be calculated by using the molar ratio of phosphate group to glucose unit as follows:

$DS = (162 + M) \times C/(M + C)$, where 162 stands for relative molecular mass of one monosaccharide residue, M represent the molar mass of PO_3H_2, and C the content of PO_4^{3-}. DS of PTTP-1 was calculated 0.43. The above result showed that phosphorylation modification was successfully carried out.

Previously, the most reliable reaction mechanism using sodium trimetaphosphate proposed by Lim and Seib mainly focused on the preparation of phosphorylated starch [25]. More recently, this reaction mechanism by sodium trimetaphosphate was improved by Lack et al [26], including alcoholate formation, opening of the sodium trimetaphosphate ring and crosslinking. Moreover, the accepted reaction mechanism by sodium tripolyphosphate was that running the esterification of sodium tripolyphosphate with polysaccharides to form phosphomonoester and phosphomonoester esterified with sodium tripolyphosphate to form phosphodiester [27]. Notably, Lim and Seib [25] investigated the preparation of phosphorylated starch and reported that a mixture of phosphate salts, including sodium trimetaphosphate and sodium tripolyphosphate, gave better results than using sodium trimetaphosphate alone to prepare derivative.

3.1. FTIR of TPP-1 and PTPP-1

The TPP-1 and PTPP-1 had little difference in waveform, wave numbers, absorption peak intensity, or peak width. The stretching vibration peak at 1140/cm indicated that PTPP-1 had pyran-type glucosidic bond [28]. Besides, the stretching vibration peak of -CH_2 at 2920/cm, the stretching vibration peak of C=O at 1640/cm and the stretching vibration peak of C-O at 1410/cm showed no significant difference between TPP-1 and PTPP-1, which shows that the fundamental structure of TPP-1 did not change after phosphorylated modification [23,29,30]. Compared with the spectrum of TPP-1, there are still two characteristic absorption peaks in the spectrum of PTPP-1 at 1232/cm and 976/cm respectively, probably caused by stretching vibration of P=O and P-O-C [28]. The FTIR spectrograms of TPP-1 and PTPP-1 are in Supporting Information.

3.2. NMR spectra of TPP-1 and PTPP-1

Previous reports by He et al. [22] and Liu et al. [13] indicated that the signals of ^{13}C NMR disappeared or weakened which might reveal adjacent −OH was substituted by phosphate group. ^{13}C NMR chemical shifts of TPP-1 were identified and shown in Table 1. Compared with TPP-1, it is noteworthy that signals at δ 60.52 ppm, 69.49 ppm, and 66.32 ppm were significantly weakened in PTPP-1, possibly indicating that C-6 of →4)-α-D-Man*p*-(1→, C-6 of →1)-α-D-Glc*p* and C-4 of→6)-α-D-Gal*p*-(1→ were phosphorylated. Unsubstituted hydroxyl at C-6 had weak steric hindrance effect and did not participate in hydrogen bond formation. Therefore substitution at C-6 of →4)-α-D-Man*p*-(1→ and C-6 of →1)-α-D-Glc*p* was more

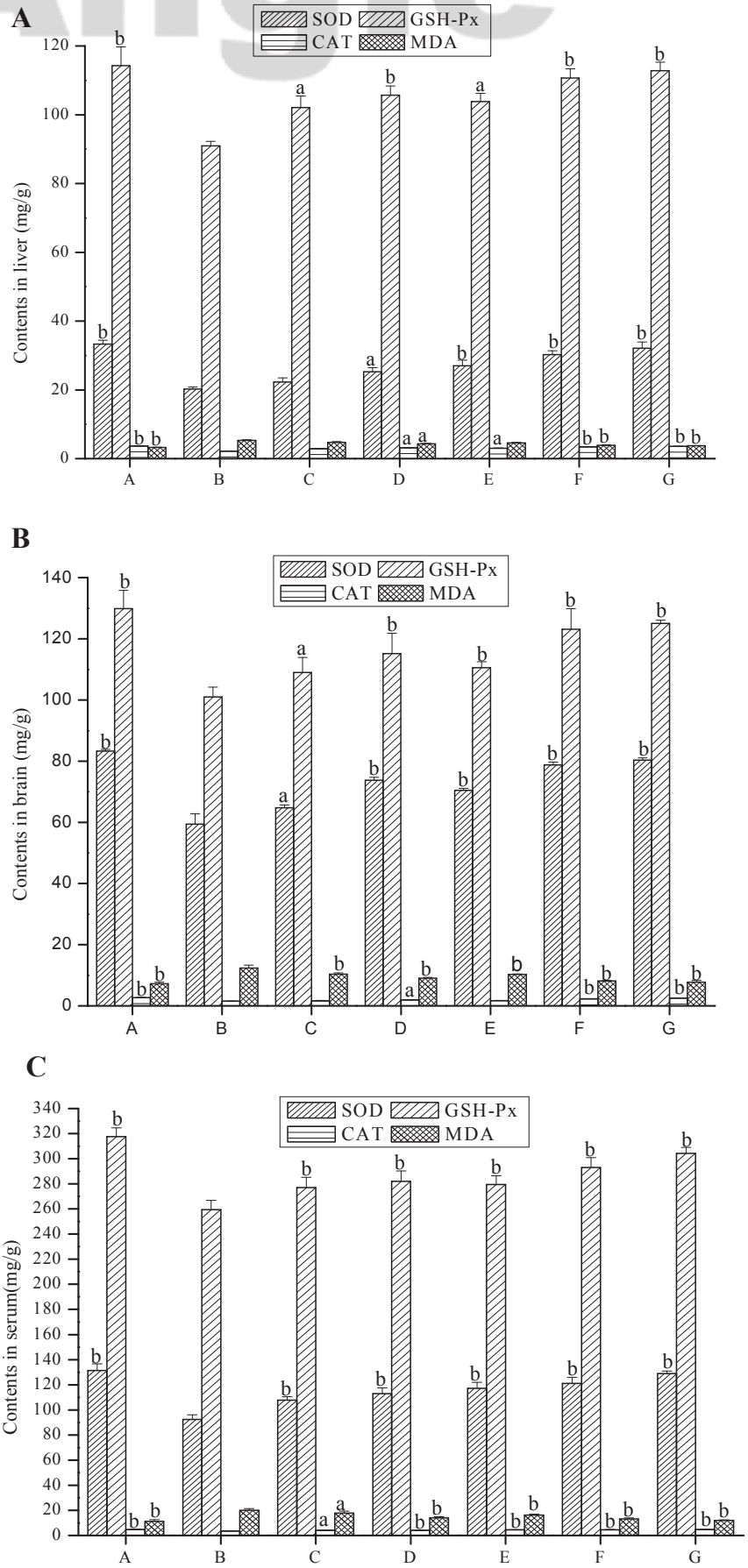

feasible. And C-4 of →6)-α-D-Gal*p*-(1→ was substituted, probably related to weak steric hindrance effect [26]. The ^{13}C NMR spectrograms of TPP-1 and PTPP-1 are provided in Supporting Information.

Moreover, the signals at δ 82.23 ppm, 76.28 ppm, and 80.81 ppm weakened slightly after modification, and might reveal that C-2 of →1)-α-L-Ara*f*, C-3 of →1)-α-L-Ara*f* and C-2 of →1)-α-L-Ara*f* -(3→ had been phosphorylated, respectively. The weakened chemical shift of C-3 of →1)-α-D-Glc*p* at δ 75.91 ppm was also considered to prove that phosphorylation was performed. It is likely that terminal residues, such as →1)-α-L-Ara*f* and →1)-α-D-Glc*p*, could be substituted on due to weak steric hindrance effect.

Besides, ^{31}P NMR spectrum of the phosphorylated derivative exhibited an intense and multisignal peaks for phosphorus resonance in the region of 0.40–2.50 ppm [31]. It was obvious that PTPP-1 showed intensive multiple signal resonance peaks at 0.95–1.73 ppm, which suggests that TPP-1 was modified successfully by phosphorylation in agreement with the result of ^{13}C NMR described above [30]. The ^{31}P NMR spectrogram of PTTP-1 was provided in Supporting Information.

In conclusion, phosphate groups in PTPP-1 might be mainly connected to C-6 of →4)-α-D-Man*p*-(1→, C-4 of →6)-α-D-Gal*p*-(1→, C-2 and C-3 of →1)-α-L-Ara*f*, C-2 of →1)-α-L-Ara*f* -(3→, C-6 and C-3 of →1)-α-D-Glc*p*, respectively. And the proposed structure of PTPP-1 is shown in Figure 2.

3.3. *Antiaging effect of TPP-1 and PTPP-1 on D-galactose-induced aging mice*

The mechanism of D-galactose-induced aging mice was that excessive D-galactose was reduced to galactitol, which cannot be metabolized and accumulates in the cell, thereby affecting the normal osmotic pressure, causing cell swelling and dysfunction, and leading to aging and metabolic disorders [2].

During the metabolic disorders process, D-galactose might induce production of excessive free radicals and initiation of lipid peroxide, which could damage the antioxidant defense system of the body [32]. After being injected with D-galactose for 6 consecutive weeks, the mice showed significant aging features, such as depressed mental state, dim and bristling fur, and significantly decreased movement, indicating that the D-galactose-induced aging mice model was established. After being gavaged for 4 weeks, compared to negative control group, body weight in low- and high-dose TPP-1 groups increased at different degrees (Table 2) and the growth in low- and high-dose PTPP-1 groups increased more significantly. Therefore, it can be concluded that PTPP-1 could significantly ($p < 0.01$) enhance the growth rate slowed by D-galactose.

Thymus and spleen are important immune organs of body and are closely associated with the differentiation, development, and cancerization processes at the molecular and cellular levels [33]. Compared with negative control group, thymus, liver, heart, kidney, and spleen indexes in low- and high-dose TPP-1 groups showed increased at different degrees, which might be due to the fact that TPP-1 could facilitated the generation of T lymphocytes and enhanced the thymus index of mice [34]. An especially interesting point was that the thymus, liver, heart, kidney, and spleen indexes in low- and high-dose PTPP-1 groups were higher than those in TPP-1 groups. All these results indicate that TPP-1 and PTPP-1 could delay the senescence of the immune organs of the D-galactose-induced aging mice and contribute to their immune functions.

The main reason for human senescence is the constantly generated free radicals during the cellular metabolism process. Excessive free radicals may bring severe damage to human body through lipid peroxidation reaction etc. When the accumulated injury brought by free radicals goes beyond the repair capacity of the body, aging of the body will occur. MDA is the product of the lipid peroxidation of the body and its content reflects indirectly the content of free radicals in body. SOD, GSH-Px, and CAT are important antioxidases in the body and they can remove the surplus free radicals in the body and thus safeguard the physiological equilibrium and prevent the damage to the body by free radicals. They play important roles for the body to fight against oxidation and damages by free radicals [24].

Compared with the negative control group, the activities of SOD, GSH-Px, and CAT in TPP-1 groups, PTPP-1 groups, and the positive control group of the liver, brain, and serum were greatly enhanced and the content of MDA significantly decreased (Figure 3). The activities of SOD in liver homogenate, cerebral homogenate, and serum of PTPP-1 high-dose group (compared with negative control group) increased by 49.55%, 33.16%, and 31.23% respectively. Activities of GSH-PX were increased by 21.68%, 21.91%, and 12.97% respectively, while CAT activity increased by 56.56%, 46.45%, and 28.22%, and the MDA content was decreased by 26.50%, 34.14%, and 33.63% respectively. All these results show that TPP-1 had significant antiaging activity and the activity of polysaccharide could be enhanced after phosphorylation. It has been reported that bioactivities of the polysaccharides are related to molecular weight, configuration of glycosidic linkages, branching degree, presence of functional groups, and monosaccharide composition, because the structural characteristic can influence the direct contact between the polysaccharides and the cells or other components of the body system [13,14].

4. Conclusion

PTPP-1 was obtained from TPP-1 by phosphorylation modification with the PO_4^{3-} content of 14.36%. The FTIR, ^{13}C NMR,

Figure 3 – Effects of polysaccharides on superoxide dismutase (SOD), glutathione peroxidase (GSH-PX), and catalase (CAT) activities and malondialdehyde (MDA) contents in (A) liver, (B) brain, and (C) serum of aging model mice. A = normal control group; B = negative control group; C = low-dose of TPP-1 group; D = high-dose of TPP-1 group; E = low-dose of PTPP-1 group; F = high-dose of PTPP-1 group; G = positive control group.

and ^{31}P NMR results indicate that the original basic structure of the polysaccharide did not change and the -H_2PO_3 groups might be connected to C-6 of →4)-α-D-Man*p*-(1→, C-6 of →1)-α-D-Glc*p*, C-4 of →6)-α-D-Gal*p*-(1→, C-2 and C-3 of →1)-α-L-Ara*f*, C-2 of →1)-α-L-Ara*f* -(3→, and C-6 and C-3 of →1)-α-D-Glc*p*. *In vivo* antiaging experiments showed that TPP-1 could greatly enhance the body weight, thymus, liver, heart, kidney, and spleen indexes, enhance the SOD, GSH-PX, and CAT levels, and reduce the MDA content in the liver, brain, and serum of aging model mice. Therefore, it was clear that TPP-1 and PTPP-1 had distinct antiaging activity. Moreover, PTPP-1 showed greater enhancement of antiaging activity compared with TPP-1 at the same dosage. In this study, TPP-1 and its derivatives could be developed as new and potential health-care products or medicines for aging prevention. The mechanism of antiaging effect of TPP-1 and PTPP-1 might be related to their antioxidation and immunoregulation abilities, whereas the exact mechanism warrant further studies.

Conflicts of interest

The authors declare no competing financial interest.

Acknowledgments

This work was financially supported by the National Natural Science Foundation of China (No. 31470146) and Scientific and Technological Research Foundation of Anhui Province of China (No. 12010302071).

Appendix A. Supplementary data

Supplementary data related to this article can be found at http://dx.doi.org/10.1016/j.jfda.2016.12.013.

REFERENCES

[1] Qiu X, Brown K, Hirschey MD, Verdin E, Chen D. Calorie restriction reduces oxidative stress by SIRT3-mediated SOD2 activation. Cell Metab 2010;12:662–7.
[2] Cui JJ, Yuan JF, Zhang ZQ. Anti-oxidation activity of the crude polysaccharides isolated from *Polygonum cillinerve* (Nakai) Ohwi in immunosuppressed mice. J Ethnopharmacol 2010;132:512–7.
[3] Ho YS, So KF, Chang RCC. Anti-aging herbal medicine—how and why can they be used in aging-associated neurodegenerative diseases? Ageing Res Rev 2010;9:354–62.
[4] Luo Q, Li Z, Yan J, Zhu F, Xu RJ, Cai YZ. *Lycium barbarum* polysaccharides induce apoptosis in human prostate cancer cells and inhibits prostate cancer growth in a xenograft mouse model of human prostate cancer. J Med Food 2009;12:695–703.
[5] Cao J, Wang J, Wang S, Xu X. *Porphyra* species: a mini-review of its pharmacological and nutritional properties. J Med Food 2016;19:111–9.
[6] Hwang PA, Hung YL, Chien SY. Inhibitory activity of *Sargassum hemiphyllum* sulfated polysaccharide in arachidonic acid-induced animal models of inflammation. J Food Drug Anal 2015;23:49–56.
[7] Liu C, Liu Q, Sun J, Jiang B, Yan J. Extraction of water-soluble polysaccharide and the antioxidant activity from *Semen cassiae*. J Food Drug Anal 2014;22:492–9.
[8] Yang S, Jin L, Ren X, Lu J, Meng Q. Optimization of fermentation process of *Cordyceps militaris* and antitumor activities of polysaccharides *in vitro*. J Food Drug Anal 2014;22:468–76.
[9] Wang CY, Wu TC, Hsieh SL, Tsai YH, Yeh CW, Huang CY. Antioxidant activity and growth inhibition of human colon cancer cells by crude and purified fucoidan preparations extracted from *Sargassum cristaefolium*. J Food Drug Anal 2015;23:766–77.
[10] Zhong L, Wang ZF, Wen DJ. Experimental research on the anti-aging effects of *Astragalus* polysaccharides. Chinese J Appl Physiol 2013;29:350–2.
[11] Yi R, Liu XM, Dong Q. A study of *Lycium barbarum* polysaccharides extraction technology and its anti-aging effect. Afr J Tradit Complem 2013;10:171–4.
[12] Tang T, He B. Treatment of D-galactose induced mouse aging with *Lycium barbarum* polysaccharides and its mechanism study. Afr J Tradit Complem 2013;10:12–7.
[13] Liu XX, Wan ZJ, Shi L, Lu XX. Preparation and antiherpetic activities of chemically modified polysaccharides from *Polygonatum cyrtonema* Hua. Carbohydr Polym 2011;83:737–42.
[14] Sinha S, Astani A, Ghosh T, Schnitzler P, Ray B. Polysaccharides from *Sargassum tenerrimum*: structural features, chemical modification and anti-viral activity. Phytochemistry 2010;71:235–42.
[15] Hu M, Hu WW. Research on the phosphate esterification of *Konjac* glucomannan. Nat Prod Res Dev 1990;2:8–14.
[16] Inoue K, Kawamoto K, Nakajima H, Kohno M, Kadoya S, Mizuno D. Chemical modification and antitumor activity of a D-manno-D-glucan from *Microellobosporia grisea*. Carbohydr Res 1983;115:199–208.
[17] Williams DL, McNamee RB, Jones EL, Pretus HA, Ensley HE, Browder IW, Di Luzio NR. A method for the solubilization of a (1→3)-β-D-glucan isolated from *Saccharomyces cerevisiae*. Carbohydr Res 1991;219:203–13.
[18] Chen SF, Huang SW, Wang CL. *Trichosanthes* phytochemical research. Chinese Tradit Pat Med 2006;28:1187–92.
[19] Moon SS, Rahman AA, Kim JY, Kee SH. Hanultarin, a cytotoxic lignan as an inhibitor of actin cytoskeleton polymerization from the seeds of *Trichosanthes kirilowii*. Bioorg Med Chem 2008;16:7264–9.
[20] Chung YB, Lee CC, Park SW, Lee CK. Studies on antitumor and immunopotentiating activities of polysaccharides from *Trichosanthes* rhizome. Arch Pharm Res 1990;13:285–8.
[21] Ye M, Yuan RY, He YL, Du ZZ, Ma XJ. Phosphorylation and anti-tumor activity of exopolysaccharide from *Lachnum* YM120. Carbohydr Polym 2013;97:690–4.
[22] He Y, Ye M, Jing L, Du Z, Surahio M, Xu H, Li J. Preparation, characterization and bioactivities of derivatives of an exopolysaccharide from *Lachnum*. Carbohydr Polym 2015;117:788–96.
[23] Sun X, Pan DD, Zeng XQ, Cao JX. Phosphorylation modification of polysaccharides from Enteromorpha. Food Sci 2011;24:017.
[24] Woo JY, Gu W, Kim KA, Jang SE, Han MJ, Kim DH. *Lactobacillus pentosus* var. *plantarum* C29 ameliorates memory impairment and inflammaging in a D-galactose-induced accelerated aging mouse model. Anaerobe 2014;27:22–6.
[25] Lim S, Seib PA. Location of phosphate esters in a wheat starch phosphate by ^{31}P nuclear magnetic resonance spectroscopy. Cereal Chem 1993;70:145–52.

[26] Lack S, Dulong V, Picton L, Le CD, Condamine E. High-resolution nuclear magnetic resonance spectroscopy studies of polysaccharides crosslinked by sodium trimetaphosphate: a proposal for the reaction mechanism. Carbohydr Res 2007;342:943–53.
[27] Tian L, Liu Y. Preparation of wheat starch phosphated with sodium tripolyphosphate. Technol Dev Chem Ind 2005;11:11–3.
[28] Qiu T, Ma X, Ye M, Yuan R, Wu Y. Purification, structure, lipid lowering and liver protecting effects of polysaccharide from *Lachnum* YM281. Carbohydr Polym 2013;98:922–30.
[29] Zou S, Zhang X, Yao W, Niu Y, Gao X. Structure characterization and hypoglycemic activity of a polysaccharide isolated from the fruit of *Lycium barbarum* L. Carbohydr Polym 2010;80:1161–7.
[30] Huang Q, Zhang L. Preparation, chain conformation and anti-tumor activities of water-soluble phosphated (1→3)-α-D-glucan from *Poria cocos* mycelia. Carbohydr Polym 2011;83:1363–9.
[31] Chen X, Xu X, Zhang L, Zeng F. Chain conformation and anti-tumor activities of phosphorylated (1→3)-β-D-glucan from *Poria cocos*. Carbohydr Polym 2009;78:581–7.
[32] Cui XU, Zuo P, Zhang Q, Li X, Hu Y, Long J, Liu J. Chronic systemic D-galactose exposure induces memory loss, neurodegeneration and oxidative damage in mice: protective effects of r-α-lipoic acid. J Neurosci Res 2006;83:1584–90.
[33] Chi HC. The effect of Chinese medicine polysaccharide on anti-aging. Heilongjiang Chinese Med 2013;2:46.
[34] Qiu MZ, Fu SC, Zhou WP, Du LF, Yang J, Dai Q. The immune regulation of polysaccharides extracted from *Lctarius deliciosus* mycelium on mice. Heilongjiang J Anim Husbandry Vet 2010;23:61.